Surface & Coatings Technology 509 (2025) 132162

Contents lists available at ScienceDirect

Surface & Coatings Technology

journal homepage: www.elsevier.com/locate/surfcoat

Chemical state depth distribution of boron in high-dose implanted iron surface

V. Takáts [a], T. Fodor [a], Z.T. Gaál [a,b], Z. Halász [a], J. Hakl [a], S. Molnár [a], A. Csík [a], G.U.L. Nagy [a,c], M. Sortica [c], J. Oscarsson [c], D. Primetzhofer [c], M. Benke [d], I. Rajta [a], K. Vad [a,*]

[a] HUN-REN Institute for Nuclear Research, H-4026 Debrecen, Bem tér 18/C, Hungary
[b] University of Debrecen, Doctoral School of Physics, 4032 Debrecen, Egyetem tér 1, Hungary
[c] Uppsala University, Uppsala, Sweden
[d] University of Miskolc, H-3515 Miskolc-Egyetemváros, Hungary

ARTICLE INFO

Keywords:
Iron boride
Surface boriding
Boron implantation
Chemical states of boron
Depth distribution of chemical states

ABSTRACT

The resistance to wear and chemical corrosion of iron surfaces can be improved by surface boriding which is commonly achieved by the powder-pack boriding method, where the iron sample is embedded in a powder of high boron concentration and heat-treated in a furnace. The boron atoms from the powder diffuse into the iron by thermal excitation, resulting in a boron concentration gradient and a bilayer comprised of two distinct boride phases FeB and Fe_2B. These phases possess different crystal structures and different thermal expansion coefficients, which leads to mechanical instability and spalling of the surface layer. In order to avoid the dual-phase structure, the boron was introduced into our samples by ion implantation, a non-diffusion-based method that can also be temperature-controlled. In this paper we report our new results of high-dose boron implantation of iron. Boron ions were implanted at a nominal fluence of $6.9{\cdot}10^{17}$ ion/cm^2 into the surface of polycrystalline iron sheets at 25 keV kinetic energy and at room temperature. After implantation, a thermal annealing was applied at the temperature of 400 °C for 1 h. The surface layer of samples was characterized by depth profile analyses of chemical constituents and of chemical states before and after annealing. We observed that when the implantation dose was high enough to produce an amorphous layer, the chemical bonds between Fe and B atoms were mainly FeB type. It was shown experimentally that these FeB chemical bonds were transformed into Fe_2B bonds by high temperature annealing. The crystalline structure of the samples wase analysed by X-ray diffraction measurements which support our findings: freshly-implanted samples only contain FeB, annealed samples contain both Fe_2B, and FeB.

1. Introduction

Surface boriding of iron and steels is a suitable technique for increasing the wear, chemical and corrosion resistances of these metals. One of the most common procedures for surface boriding is the thermochemical surface treatment called powder-pack boriding [1], where the sample is embedded in a powder of high boron concentration, usually boron-carbide, and annealed at high temperature, causing boron atoms of the powder to diffuse into the iron. The influx of boron modifies the chemical composition of the surface layer, resulting in an outer FeB phase with higher boron concentration and an inner Fe_2B phase with lower boron concentration. The dual-phase forms an unavoidable boron concentration gradient along the diffusion path (boron concentration decreases with depth) and has undesirable consequences. The two boride phases have different crystal structures and thermal expansion coefficients. The thermal expansion coefficient in the more brittle FeB phase is about three-fold higher than in the Fe_2B phase [2,3]. These differences lead to cracks at the interface between the two phases and to spalling of the iron boride layer [4–6]. Industrial applications require the protective boride layer to be contiguous and tough against both mechanical and chemical exposure, while the coated item or tool in question must retain its well-defined size and shape.

One solution which meets this prerequisite is the ion implantation, a non-chemical and non-diffusion-reliant procedure of surface boriding. The aim of this work is to prove that ion implantation is a possible candidate for surface boriding. Boron ions were implanted into iron and

* Corresponding author.
E-mail address: vad@atomki.hu (K. Vad).

https://doi.org/10.1016/j.surfcoat.2025.132162
Received 30 January 2025; Received in revised form 11 April 2025; Accepted 11 April 2025
Available online 16 April 2025

depth distribution of elements and their chemical states was investigated. It is also important to answer the question whether the boride layer formed by ion implantation is a monophase layer, or a double-phase layer of FeB and Fe_2B, because in the latter case the implanted layer does not have good chemical and wear resistances.

Boron implantation into iron surface is not a novel method. In 1975 Takagi et al. showed that ion implantation can be used to modify iron surfaces effectively [7]. They implanted boron ions into iron by low kinetic energy (10–25 keV) and experienced a marked increase in the surface hardness without any change in magnetic properties. The analysis of transmission electron diffraction patterns of samples annealed for 1 h at 500 °C showed the existence of both FeB and Fe_2B phases in the implanted layer. Amorphous phases of iron boride layers prepared by implantation and melt spinning were compared and the results showed that a completely amorphous layer could not be achieved by implantation [8]. Application of ion implantation for surface modification was also studied by Hartley [9]. The author obtained that boron implantation intensively improved the tribological properties of steel and metal surfaces, especially when high-dose implantation was applied [10].

Chemical bonds between boron and iron atoms were studied by X-ray photoelectron spectroscopy in samples which were synthesized at high temperatures from iron and boron powders [11]. Another important photoelectron spectroscopy work highlighted that the chainlike structure of boron atoms in FeB is the result of strong covalent B—B bonding, while B—B bonding in Fe_2B is not as strong as in FeB [12]. The binding energies belonging to the boron 2 s, 2p states of the two compounds are different, and the $2sp^2$ hybridization bands that they form also show binding energy differences. The paper by Joyner [12] shows that in case of Fe_2B there is a shift in the binding energies towards the Fermi level due to the crystal structure transformation. However, to the best of our knowledge, neither the depth distribution of chemical bonds between iron and implanted boron atoms nor the changes they undergo at high temperatures have been studied.

The purpose of our research work was twofold. First, to prepare a single-phase boride layer by a method different from thermo-chemical procedure. Secondly, to understand the ion implantation mechanism and to answer the question of what type of chemical interaction should be to form a metastable disordered structure of the iron matrix and implanted ions. In this work, boron ions were implanted into iron sheets and depth distributions of boron chemical bonds were analysed by photoelectron spectroscopy before and after annealing at a high temperature. We discussed three questions: what are the chemical bonds after implantation, what is the depth distribution of these chemical bonds, and what is the effect of annealing on them.

2. Sample preparation and experimental arrangement

In our experiments pure iron sheets (99.99 %) were implanted by boron ions at room temperature. The irradiated iron sheets were 10x10x0.8 mm in size. The implantation was carried out by ^{11}B ions of 25 keV kinetic energy, with a nominal dose of 6.9×10^{17} ion/cm^2. During implantation, the sample was kept close to room temperature by a water-cooled sample holder. The depth distribution of implanted boron ions in iron sheets was studied by secondary neutral mass spectrometry (SNMS) depth profiling. SNMS is similar to secondary ion mass spectrometry (SIMS). The sample surface is sputtered by Ar^+ ions, but instead of secondary ions, neutral particles which escaped from the surface are detected by post-ionization [13,14]. The kinetic energy of Ar^+ ions applied for surface irradiation was 350 eV.

Crystalline structures of samples were checked by X-ray Diffraction (XRD) analyses. The problem with XRD is that it is not a surface sensitive technique. The X-ray penetrates deep into the material (1–100 μm) and is scattered from both the surface and the bulk. Since in our experiments the change in the structure of the surface layer is important, one of the main requirements for XRD analyses is the reduction of X-ray scattering from the bulk in order to maximise the signal from the surface layer. The solution to this problem is the use of grazing-incidence X-ray irradiation because in this arrangement the penetration depth is confined to the surface layer. If the angle between the incident X-ray and the sample surface plane is below a critical value, the X-ray suffers total reflection on the surface (this is the total reflection angle which is about 0.5°) [15]. Thus, the incidence angle of the X-ray must be just above the total reflection angle. In surface analyses arrangement the incidence angle of X-ray is constant and the scattering angle (2Θ) is scanned. In our XRD analyses 0.7° was chosen as the incidence angle.

Chemical bonds between constituents were analysed by X-ray Photoelectron Spectroscopy (XPS). The measurements were performed with a dual-anode non-monochromatized X-ray source and a hemispherical type energy analyser (SPECS, Berlin, Germany). The base vacuum in the instrument was better than 10^{-9} mbar, while during measurement it stayed better than 10^{-8} mbar. Spectra were sequentially recorded using Mg Kα radiation (1253.6 eV) at 10 kV acceleration voltage and 20 mA emission current. The binding energy scale was calibrated by Au $4f_{7/2}$ and Cu $2p_{3/2}$ peaks obtained from a freshly sputter-cleaned sample containing both metals, as prescribed by the manufacturer. Charge referencing was done by the metal decoration technique, using copper as the reference material. Spectra were processed with the software CasaXPS (http://www.casaxps.com/).

An advantage of our experimental arrangement is that the vacuum systems of the mass spectrometer and the XPS instrument form a joint vacuum chamber that allows sample transfer between instruments under ultrahigh vacuum conditions, with no exposure to the atmosphere for the entire duration of the measurements. The cross section of the implanted layer was revealed by mechanical polishing and was investigated by a scanning electron microscope (SEM), type JEOL JSM-IT500HR. The samples were measured in nitrogen gas of 70 Pa pressure for charge compensation.

3. Results and discussion

SEM images of the implanted boride layer show uniform layer thickness. The near surface cross-sections of the samples before and after implantation are presented in Fig. 1. The saw-tooth morphology typically observed in samples prepared by powder-pack boriding is not present. The uniform layer thickness is important for wear and chemical resistances when the thickness is below 1 μm. The layered structure of the sample surface was revealed by SNMS. The depth profiles of B and Fe in the surface region of a freshly implanted sample are shown in Fig. 2. The blue curve shows the iron depth distribution. At 25 keV kinetic energy of implanted ions, inelastic collisions dominate between the ions and lattice atoms [16]. Therefore, the decrease in iron concentration in Fig. 2 between 10 and 180 nm was not a result of atomic displacements, it was rather the result of volume expansion of the mixed layer. Low implantation energy was chosen to produce a shallow implanted layer. It can be seen in Fig. 2 that the boron is present in the topmost 250 nm thickness of the sample.

High implantation dose was required mainly to yield the high boron concentration needed to facilitate proper high-resolution XPS measurement of the *B* 1s peak, to which the method is relatively insensitive. In case of high-dose implantation the distribution of implanted ions is rather a Pearson-type than Gaussian-type [17] and the implanted ions form an amorphous phase with the host matrix [18]. The question arose whether this amorphous phase is reflected in the depth distribution of implanted particles. Plotting the ratio of B/Fe vs. B in a log-log scale coordinate system, where B and Fe denote the experimentally measured intensities of boron and iron, the data show linear dependence in the low concentration region near the maximum penetration depth of B ions (Fig. 3). The reason of this is that near the maximum penetration depth, where boron intensity was low approaching the zero, the crystalline structure of the host iron matrix suffered only deformation. The number of iron atoms remained constant at increasing boron intensity. Beyond the ratio of B/Fe = 0.15 when boron intensity $>10^4$ cps (dashed line in

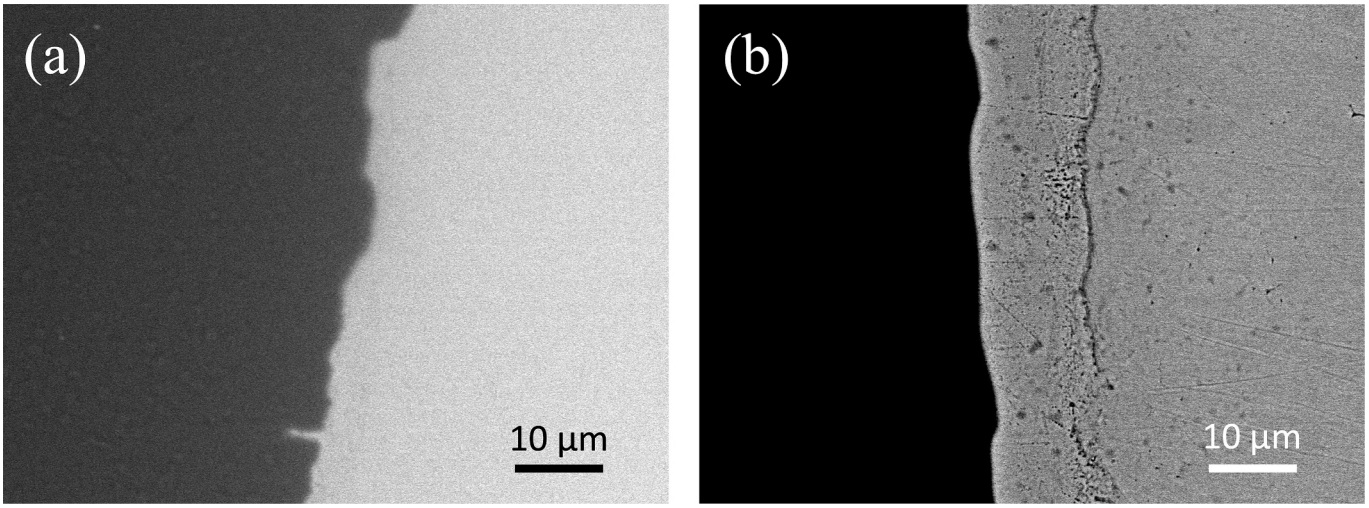

Fig. 1. SEM cross-sectional views of surface layer (a) before implantation (b) after implantation. The cross-section of the implanted layer was not perpendicular to the implantation surface. Therefore, the thickness of the implanted layer in the SEM image looks higher than reality.

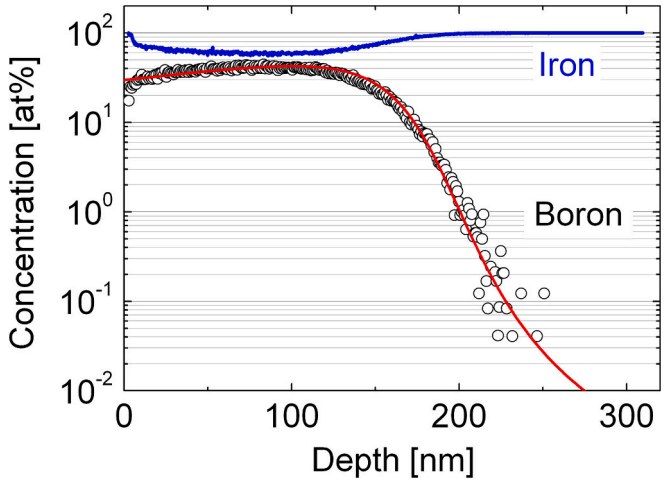

Fig. 2. Boron and iron depth distributions in the surface layer of an iron sample implanted by boron ions of 25 keV with a dose of $6.9 \cdot 10^{17}$ ion/cm^2. The red line is the calculated boron concentration made by the type-IV distribution of Pearson curves [17].

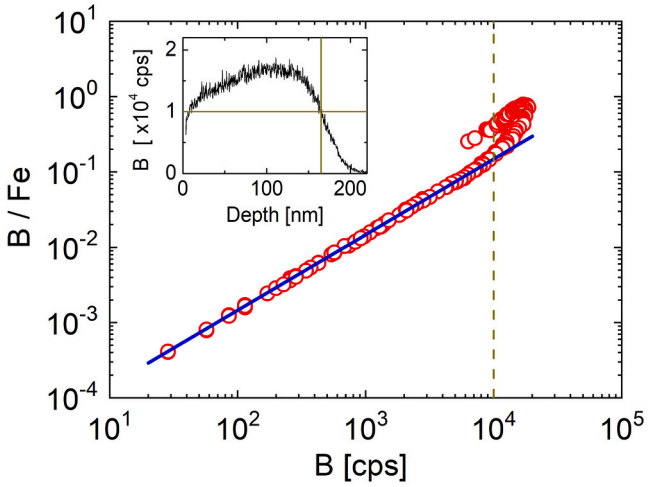

Fig. 3. Dependence of the B/Fe ratio on the intensity of B. The red circles are the experimental data, the blue line is the linear fitting. The dashed line marks the depth of the threshold boron concentration. The inset shows the depth distribution of the implanted boron. The cross lines help to find the depth belonging to 10^4 cps boron intensity.

Fig. 3), experimental data deviate from the line. The explanation of this is that at the point of B/Fe = 0.15 the iron matrix deformation evoked the collapse of the crystalline structure. The boron fluence that belongs to this point is a threshold fluence. Below the threshold fluence the implanted layer has a disordered crystalline structure and beyond the threshold fluence this crystalline structure alters into a metastable amorphous phase.

The inset of Fig. 3 shows the depth distribution of boron intensity. It can be seen that the intensity of 10^4 cps belongs to the depth of 165 nm, i.e., this depth can be considered a phase border between the metastable amorphous phase and the deformed crystalline structure in the implanted layer. If the depth is lower than 165 nm, the layer structure is amorphous, while the deeper layer is formed by deformed crystalline structure.

If the ratio of B/(B + Fe) is plotted instead of B/Fe, the linear range of the experimental curve in log-log scale expands into the direction of higher boron concentration due to the increase of the denominator of this ratio. The maximum concentration of the linear range where the disordered crystal structure becomes amorphous is 20 %. This is the phase border between the two phases. The amorphous structure of implanted $Fe_{1-x}B_x$ films, where x denotes the concentration of implanted boron ions, was studied in the paper of Ref. [19] by transmission electron microscopy and resistivity measurements. The authors experienced that the film was amorphous, if the implanted boron concentration is higher than 20 %.

The amorphous phase fraction of the implanted layer depends on the concentration of implanted ions. When boron concentration is near 40 %, as in our samples, most of the layer is in amorphous state [8]. The dependence of iron boride phases on the temperature and implantation dose was studied in the paper of Rauschenbach et al. [20]. According to this paper, the crystal structure of the implanted layer of our samples was expected to be amorphous. In order to check it, the layer was characterized by XRD. Fig. 4a shows the XRD pattern of the implanted layer of as-prepared samples. The lack of intense peaks in the diffraction pattern suggests that most of the implanted layer was indeed in amorphous state, only a small fraction remained crystalline. This fraction was the deeper layer of the implantation where the boron concentration was below the threshold fluence.

The amorphized phase of the implanted layer could be re-crystallized

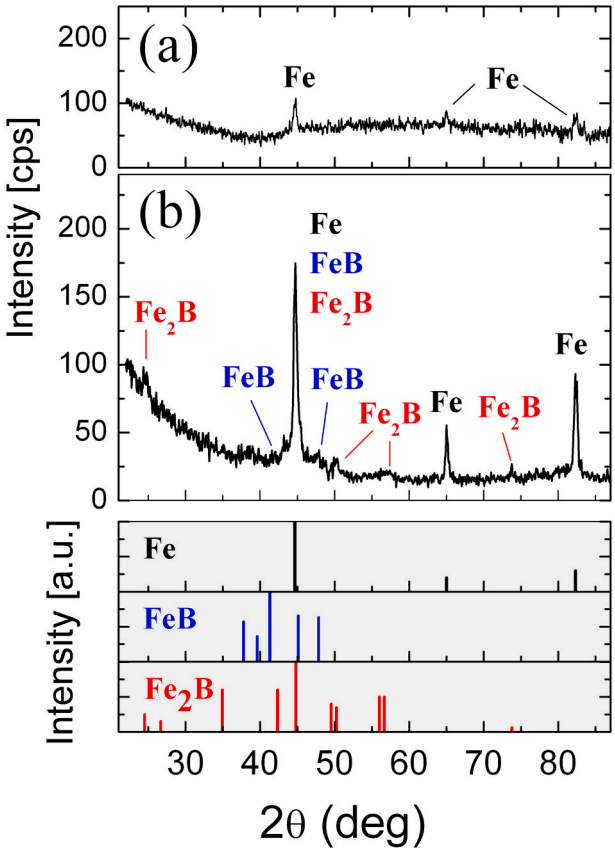

Fig. 4. X-ray diffractograms of the implanted layer (a) before annealing; (b) after 1 h annealing at 400 °C. The bottom figure of the diffractogram (with grey background) shows the reference positions of Fe, FeB and Fe_2B reflections according to the datasheets 00-006-0696, 00-032-0463 and 01-072-1301 of ICDD database.

by thermal annealing at a given temperature. According to the phase diagram (see Fig. 2 of the paper Rauschenbach et al. [20]), 400 °C is an adequate temperature for recrystallization. As it can be seen in the phase diagram, this temperature is high enough for recrystallization, regardless of implantation dose. After annealing the samples at 400 °C for 1 h, new reflection peaks appeared on the X-ray diffraction pattern according to FeB and Fe_2B crystallites (Fig. 4b). The amorphous phase generated by implantation was a metastable formation and some thermal energy was needed to transform it to a stable crystalline structure. This raised a question. What was the chemical states between boron and iron atoms which stabilized the implantation induced amorphous phase and could be changed by thermal excitation?

The depth distribution of chemical bonds was revealed by XPS combined with surface sputtering. Between two XPS measurements, the sample was transferred into the SNMS chamber and its surface was sputtered by a low energy Ar^+ ion beam for a given time to remove ~20 nm thick layer of the sample. XPS spectra of the freshly exposed surface were then recorded. The *B* 1s photoelectrons were analysed in detail. The sputtering and analysis steps were repeated until the iron substrate was reached, i.e., until the observed boron concentration decreased below the level at which *B* 1s spectra could be reasonably evaluated. This XPS depth profiling was performed again after annealing the sample in vacuum at 400 °C for 1 h. Fig. 5 shows some representative results of XPS measurements at two depths.

It can be seen in Fig. 5 that promptly after implantation when the implanted layer was mainly amorphous, the chemical bonds were only FeB type, no Fe_2B was found. However, by annealing the sample at 400 °C for 1 h, the chemical linkages changed from FeB to Fe_2B. Moreover, this change had a depth dependent property as reflected in Fig. 6. The panels of Fig. 6 are divided into two areas, into a lighter and a darker grey area. The border between them is at the depth of 165 nm where the fluence of implanted boron drops below the threshold value. It can also be seen in Fig. 6 that in the darker grey area, where the crystal structure was merely disordered and not destroyed, the chemical bonds stayed stable at 400 °C annealing.

The concentration of FeB chemical bonds as a function of boron concentration is shown in Fig. 7. There is a break point in the linear function near 20 % of boron concentration. This break point is just at the phase border between the amorphous and crystalline structures of the iron boride layer. In the low concentration range, the number of FeB chemical bonds increases linearly with the boron concentration. Over 20 % of boron concentration the amorphous phase dominates with constant concentration of FeB chemical bonds, i.e., with the increase in

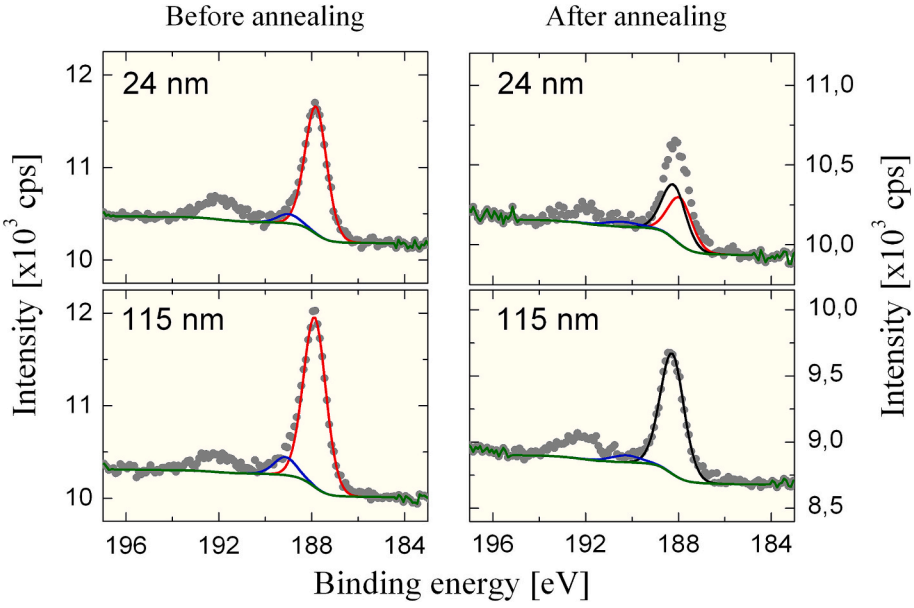

Fig. 5. *B* 1s spectra of the implanted layer at two depths, before (left) and after (right) annealing. Grey dots are the experimental data. Lines denote: red – FeB, black – Fe_2B, blue – boron-suboxide, green – background. The peak at the binding energy of 192 eV belongs to $FeBO_3$.

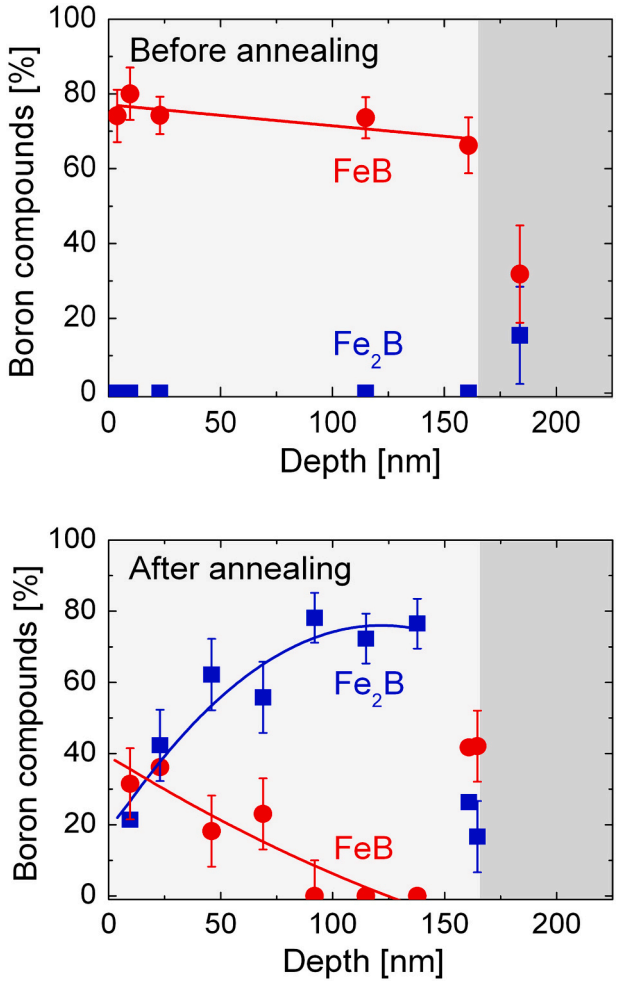

Fig. 6. Depth distributions of chemical bonds of Fe and B atoms before and after annealing at 400 °C for 1 h. The border line between the lighter and darker grey areas is at the threshold depth (165 nm).

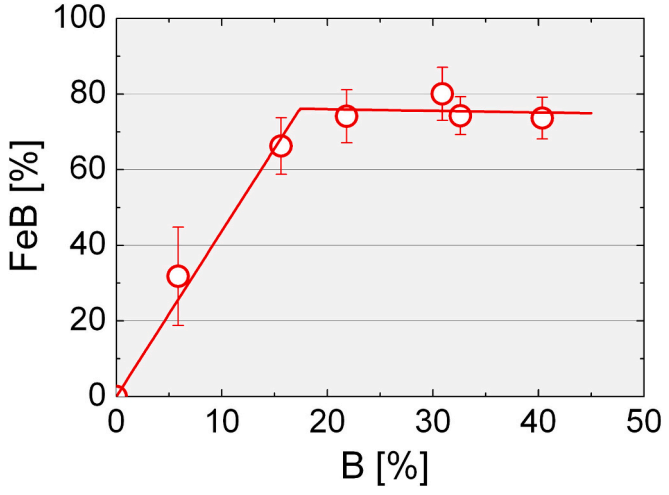

Fig. 7. Concentration of FeB in the implanted layer as a function of total boron concentration.

boron concentration, the number of FeB chemical bonds does not increase.

In addition to iron, boron ions in the implanted layer form chemical bonds with oxygen, as well. In the *B* 1s spectra two oxide peaks could be identified which belong to different compounds. In Fig. 5, the peak at the binding energy of 192 eV belongs to the compound of $FeBO_3$ and the one at 189–190 eV belongs to boron suboxides. Oxidized boron compounds were formed during the implantation and were found to be stable at 400 °C. The total oxide and suboxide content and their depth distributions were unchanged after annealing, except for the outermost surface layer where the boron suffered further oxidation. The experimental results show that about 20 % of the implanted boron forms oxides and suboxides (Fig. 8). In the strongly disordered crystalline structure, where the boron concentration was below the threshold concentration (at the depth below 165 nm), the boron oxide concentration was roughly the same as the FeB concentration (30–40 %).

4. Conclusions

Surface boriding of iron samples was produced by low energy, high-dose ion implantation. The implantation energy was 25 keV, the dose was 6.9×10^{17} ion/cm^2. The thickness of the implanted surface layer was 200 nm. Due to the high dose, the boron distribution was Pearson-type instead of Gaussian-type. The depth of the phase border between amorphous and crystalline phases in the implanted layer was also determined. The aim of this work was to obtain information about the chemical bonds between boron and iron atoms in the implanted layer and their changes due to high temperature annealing. The depth distribution of constituents in the implanted layer and of the chemical bonds were determined by SNMS depth profile analysis and XPS, while the crystal structure was examined by XRD measurements. We can conclude that the results are completely new in this field. The chemical bonds formed by implantation in the surface layer were mainly FeB, which were changed to Fe_2B by a high temperature (400 °C, 1 h) heat treatment. A phase border was identified in the implanted layer which divides it into an amorphous region and a (distorted) crystalline region. The results are important for better understanding the physical process of ion implantation and for surface modification by ion implantation. Iron boride surfaces are widely used in lead-free soldering technology. Therefore, the effects of implantation dose, implantation energy, annealing time and temperature are very important for future study.

CRediT authorship contribution statement

V. Takáts: Validation, Investigation, Conceptualization. **T. Fodor:** Writing – review & editing, Investigation. **Z.T. Gaál:** Software,

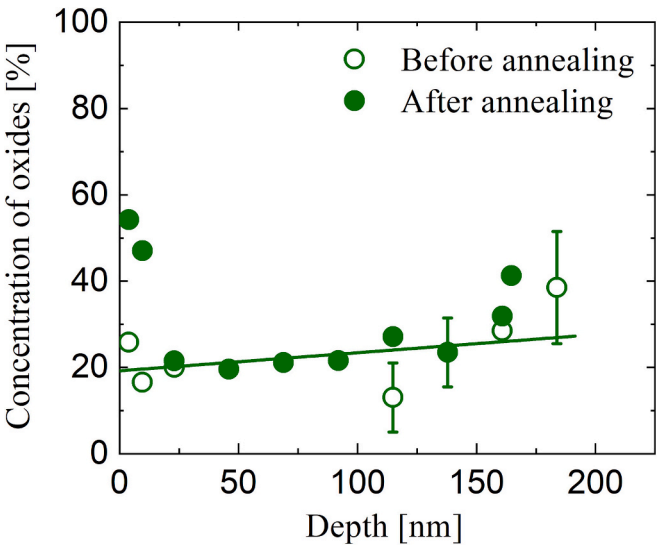

Fig. 8. Depth distribution of total concentration of oxide compounds in the implanted layer.

Investigation. **Z. Halász:** Software, Conceptualization. **J. Hakl:** Validation, Supervision. **S. Molnár:** Visualization, Investigation. **A. Csík:** Visualization, Investigation. **G.U.L. Nagy:** Investigation. **M. Sortica:** Investigation. **J. Oscarsson:** Investigation. **D. Primetzhofer:** Investigation. **M. Benke:** Conceptualization. **I. Rajta:** Resources, Methodology. **K. Vad:** Writing – review & editing, Writing – original draft, Supervision, Conceptualization.

Declaration of competing interest

The authors declare that they have no known competing financial interests or personal relationships that could have appeared to influence the work reported in this paper.

Acknowledgement

This work was supported by the project TKP2021-NKTA-42 financed by the National Research, Development and Innovation Fund of the Ministry for Innovation and Technology, Hungary. Accelerator operation at Uppsala University was supported by the Swedish research Council VR-RFI (contract #2019_00191).

Data availability

No data was used for the research described in the article.

References

[1] M. Keddam, S.M. Chentouf, A diffusion model for describing the bilayer growth (FeB/Fe2B) during the iron powder-pack boriding, Appl. Surf. Sci. 252 (2005) 393–399, https://doi.org/10.1016/j.apsusc.2005.01.016.
[2] C. Kapfenberger, B. Albert, R. Pöttgen, H. Huppertz, Structure refinements of iron borides Fe2B and FeB, Z. Kristallogr. 221 (2006) 477–481, https://doi.org/10.1524/zkri.2006.221.5–7.477.
[3] O. Ozdemir, M. Usta, C. Bindal, A.H. Ucisik, Hard iron boride (Fe_2B) on 99.97 wt% pure iron, Vacuum 80 (2006) 1391–1395, https://doi.org/10.1016/j.vacuum.2006.01.022.
[4] Y. Kayali, S. Taktak, Characterization and Rockwell-C adhesion properties of chromium-based borided steels, J. Adhes. Sci. Technol. 29 (2015) 2065–2075, https://doi.org/10.1080/01694243.2015.1052617.
[5] I.E. Campos-Silva, G.A. Rodríguez-Castro, Boriding to improve the mechanical properties and corrosion resistance of steels, in: E.J. Mittemeijer, M.A.J. Somers (Eds.), Thermochemical Surface Engineering of Steels Improving Materials Performance, Elsevier Ltd., Amsterdam, 2015, pp. 651–702, https://doi.org/10.1533/9780857096524.5.651.
[6] M. Rile, Reasons for the formation of cracks in boride coatings on steel, Met. Sci. Heat Treat. 16 (1974) 836–838, https://doi.org/10.1007/BF00664246.
[7] T. Takagi, I. Yamada, H. Kimura, Iron surface treatment by boron implantation, in: S. Namba (Ed.), Ion Implantation in Semiconductors, Science and Technology, Plenum Press, New York, 1975, pp. 335–340, https://doi.org/10.1007/978-1-4684-2151-4.
[8] J. Jagielski, M. Kopcewicz, L. Thomé, Mössbauer study of the amorphization process in α-Fe by boron implantation, J. Appl. Phys. 73 (1993) 4820–4824, https://doi.org/10.1063/1.353848.
[9] N.E.W. Hartley, Ion implantation and surface modification in tribology, Wear 34 (1975) 427–438.
[10] V.I. Lavrentiev, A.D. Pogrebjak, High-dose ion implantation into metals, Surf. Coat. Technol. 99 (1998) 24–32.
[11] V.G. Alyoshin, A.I. Kharlamov, V.M. Prokopenko, Investigation of composition and chemical state of elements in iron boride by the method of X-ray photoelectron spectroscopy, J. Solid State Chem. 38 (1981) 105–111.
[12] D.J. Joyner, R.F. Wills, Photoelectron spectroscopy of the iron borides, structures, bonding and magnetic behaviour, Philos. Mag. A 43 (1981) 815–833, https://doi.org/10.1080/01418618108240410.
[13] H. Oechsner, L. Reichert, Energies of neutral sputtered particles, Phys. Lett. 23 (1966) 90–92.
[14] K. Vad, A. Csik, G.A. Langer, Secondary neutral mass spectrometry – a powerful technique for quantitative elemental and depth profiling analyses of nanostructures, Spectrosc. Eur. 21 (2009) 13–16.
[15] G.F. Harrington, J. Santiso, Back-to-basics tutorial: X-ray diffraction of thin films, J. Electroceram. 47 (2021) 141–163, https://doi.org/10.1007/s10832-021-00263-6.
[16] J. Peltola, Stopping Power for Ions and Clusters in Crystalline Solids, Academic Dissertation, University of Helsinki, 2003, p. 10. ISBN 952-10-0940-3.
[17] D.G. Ashworth, R. Oven, B. Mundin, Representation of ion implantation profiles by Pearson frequency distribution curves, J. Phys. D Appl. Phys. 23 (1990) 870–876.
[18] P.M. Ossi, Ion-beam-induced amorphization, Mater. Sci. Eng. 90 (1987) 55–68.
[19] L. Thomé, A. Benyagoub, A. Audouard, J. Chaumont, Amorphous Fe-B alloys produced by ion implantation. I: electrical properties, J. Phys. F 15 (1985) 1229–1236.
[20] B. Rauschenbach, V. Heera, Formation of borides and nitrides by ion implantation in iron, J. Less Common Metals 117 (1986) 323–327.